

STUDIES ON 4-SULFAMOYLANILINIUM NITRATE SINGLE CRYSTALS

G.Sharmila Devi^{1*}, S.Kalyanaraman², S. Sheik Saleem³,

¹Research scholar, Reg.No. 5560, Department of Physics, Sri Paramakalyani College, Alwarkurichi-627412, Tirunelveli district, Tamilnadu, India.

(Manonmaniam Sundaranar University, Abishekapatti, Tirunelveli-627012, Tamilnadu, India)

²Associate Professor of Physics and Principal (Retd.), Department of Physics, Sri Paramakalyani College, Alwarkurichi-627412, Tirunelveli district, Tamilnadu, India.

³Associate Professor of Physics (Retd.), Department of Physics, Sri Paramakalyani College, Alwarkurichi-627412, Tirunelveli district, Tamilnadu, India.

Abstract

Salt of 4-sulfamoylanilinium nitrate (4SAN) was synthesized by using sulphanilamide and nitric acid and single crystals of the 4SAN were grown by solution method. Solubility of the sample is found to be increasing with increase of temperature. XRD study reveals that 4SAN crystal has monoclinic structure. The functional groups of the grown 4SAN crystal have been found by infrared spectral studies. Optical studies were carried out for the sample to determine band gap, extinction coefficient, absorption coefficient and reflectance. The microhardness studies of 4SAN crystal were performed to find the mechanical parameters and the results have been analysed.

Key words: NLO; single crystal; semiorganic; solution growth; XRD; FTIR; band gap; work hardening coefficient; reflectance

1. Introduction

Organic compounds are often formed by weak hydrogen and Van der Waals bonds and hence possess a high degree of charge delocalization leading to large NLO coefficients. However, organic compounds frequently suffer from volatility, poor thermal stability, poor mechanical strength and undesirable growth habits making them unattractive for device fabrication. In order to overcome these difficulties, semiorganic crystals have been proposed in which the high optical nonlinearity of purely organic compound is combined with the favourable mechanical and thermal properties of inorganics. Also they possess several attractive properties like high optical damage threshold, wide transparency range, adequate birefringence for phase matching which make them suitable for frequency doubling [1-3]. Here, a semiorganic NLO material viz., 4-sulfamoylanilinium nitrate (4SAN) was synthesized and studied. Among sulfa drug derivatives, sulfanilamide is an important one in the medical history. Aromatic sulfonamide derivatives exhibit a range of bioactivities, including anti-angiogenic anti-tumor, anti-inflammatory and anti-analgesic, anti-tubercular, anti-glaucoma, anti-HIV, antimicrobial and anti-malarial agents [4-6]. Sulfamides have been used extensively worldwide for decades and are effective antimicrobial drugs for the prevention of infections in cattle, poultry, and swine to

treat veterinary diseases, and to promote growth. Nowadays, the main use of sulfamides is in veterinary for intensive livestock production. These antibiotics and metabolites are eliminated through animal excretions and hence they are persistent in the manure liquids. One important sub-group of these antibiotics is the sulfonamides whose molecular structure has a sulfonic group joined to one amino group. The sulfone group can have joined an aromatic ring, like a 4-aminophenyl moiety, and the amino group can be monosubstituted by different groups. The sulfonamides, sulfamethoxypyridazine, sulfamethoxydiazine, sulfamethoxypyrimidine can be representative models of this drug family. These compounds are used widely in therapeutics and represent two groups of sulfonamides, sulfonamido-pyrimidines and sulfonamido-pyridazines [7-10]. Badiia Essghaier *et al.* synthesized and characterized the sample of 4-sulfamoyl-phenyl-ammonium sulphate by X-ray diffraction and other studies. This compound crystallizes in the orthorhombic system, spaces group *Pbcn*. Here it is shown that the synthetic sulfanilamide exhibits promising antibacterial potency. It is showed that the sulfanilamide sulphate had high activity against bacteria, yeast and fungi, compared to others published antifungal compounds [11]. In this investigation, single crystals of 4-sulfamoylanilinium nitrate (4SAN) were grown by aqueous solution method with slow evaporation technique. Various studies of the grown crystals of 4SAN were carried out and the results are discussed in this paper.

2. Synthesis, solubility and growth

The salt of 4-sulfamoylanilinium nitrate was synthesized by dissolving AR grade sulphanilamide and nitric acid in the stoichiometric ratio of 1:1 in double distilled water. The solution was stirred for 3 hours using magnetic stirrer and then filtered using the good quality filtered papers. The synthesized salt of 4-sulfamoylanilinium nitrate (4SAN) was extracted according to the following reaction after evaporating the solvent.



Here the anion and cation were combined to form the required salt. In solution growth technique, the size of a crystal depends on the amount of the material available in the solution which in turn is decided by the solubility of the material in that solvent. The solubility study of 4SAN sample was made at different temperatures by gravimetric method. 50 ml of double distilled water was taken in a beaker and synthesized salt of 4SAN was added step by step at room temperature and the solution was continuously stirred using magnetic stirrer. The addition of salt was done until the solution reaches the saturated state. The solute present in 25 ml of the solution was dried and weighed accurately using an electronic balance. The variation of solubility with temperature for 4SAN salt is shown in figure 1. The results indicate that the solubility increases with temperature and hence this sample has positive temperature coefficient of solubility. The solubility curve has the three regions namely saturated region, supersaturated region and undersaturated region. Above the solubility curve in the figure 1, there is the supersaturated region and below the curve, the region is called the

undersaturated region. Very close and above the solubility curve, the zone is called as the metastable zone width and in this zone, the crystal would grow and spontaneous nucleation would not be formed [12, 13]. Hence, good quality and big-sized crystals could be grown in the region of metastable zone width. In the undersaturated region, the crystal will not grow because the nucleation will not be formed in this region. 4SAN crystals were grown by slow evaporation technique using the synthesized salt of 4SAN. Saturated solution was prepared from synthesized 4SAN salt using double distilled water as solvent. The solution was continuously stirred for about 2 hours using magnetic stirrer at room temperature. The solution was filtered using Whatmann filter paper and then kept in a growth vessel covered with the perforated sheet. Big-sized crystals of 4SAN were harvested from the solution after 35 days. A grown crystal of 4SAN is shown in figure 2. The dimensions of the grown crystal of 4SAN is observed to be $11 \times 10 \times 7 \text{ mm}^3$.

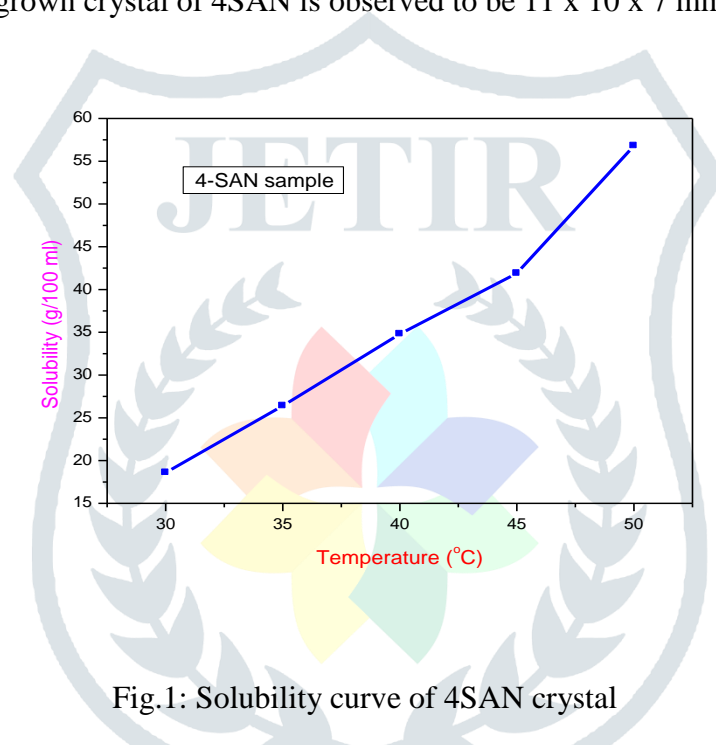


Fig.1: Solubility curve of 4SAN crystal



Fig.2: A harvested crystal of 4-sulfamoylanilinium nitrate (4SAN)

3. Identification of functional groups by FTIR method

An infrared spectrum is a fingerprint of a sample with absorption peaks which correspond to the frequencies of vibrations between the bonds of the atoms making up the material because different material is a unique combination of atoms and no two compounds produce the exact same infrared spectrum. Infrared spectrometry involves examination of twisting, bending, rotation and vibration modes of atoms in a molecule. Fourier Transform Infrared (FTIR) spectrometry was developed in order to overcome the limitations encountered with dispersive instruments. In this method, the grown crystal is finely ground and it is intimately mixed with about 100 times its weight of powdered KBr. The mixture is then pressed into a pellet using a die and the resulting pellet must be transparent to IR radiation. The quality of the pellets depends on the mixture taken, magnitude and duration of pressure, the dryness of the matrix material and the design and condition of the die [14, 15]. The FTIR spectrum (Fig.3) of the grown 4SAN crystal has been drawn in the wave number range 400-4000 cm^{-1} with Perkin Elmer Fourier transform infrared spectrometer using KBr pellet technique. The functional groups present in 4SAN crystal were identified with the help of reported data [16, 17]. The stretching vibrations of NH_2 group are observed at the absorption frequencies at 3481 and 3382 cm^{-1} . The vibration at 1630 cm^{-1} corresponds to the NH_2 bending mode. The stretching mode of NO_3^- of the molecule is noticed at 811 cm^{-1} and absorption peaks at 1138 cm^{-1} and 908 cm^{-1} are due to SO_2 stretching vibrations. The FTIR assignments to all the absorption peaks of the spectrum of 4SAN crystal are given in the table 1.

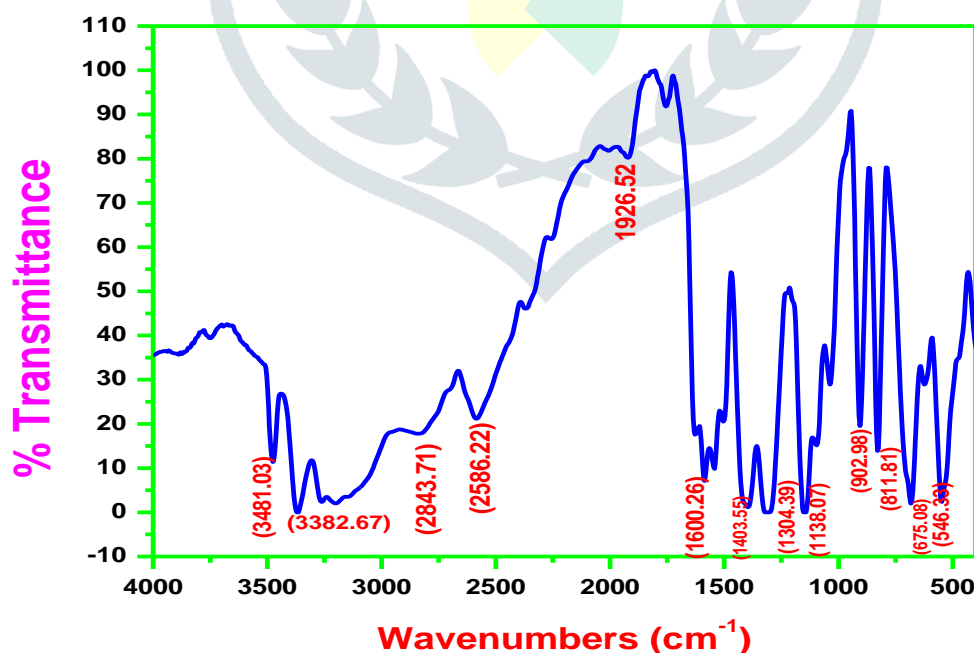


Fig.3: FTIR spectrum of 4SAN crystal

Table 1 FTIR assignments for 4SAN crystal

Wave number (cm ⁻¹)	FTIR assignments
546	NH ₂ torsion
675	C-S stretching
811	(NO ₃) ⁻ stretching
902	SO ₂ stretching
1138	SO ₂ stretching
1404	C=C stretching
1600	NH ₂ bending
1926	CH stretching (aromatic)
2586	CH stretching
2843	CH stretching
3382	NH ₂ symmetric stretching
3481	NH ₂ asymmetric stretching

4. X-ray diffraction analysis

It is known that a crystalline substance acts as a three dimensional diffraction grating for X-ray wavelengths similar to the spacing of planes of the crystal lattice. X-ray diffraction is now a common technique for the study of crystal structures and atomic spacing and it is based on constructive interference of monochromatic X-rays onto a crystalline sample. The monochromatic X-rays incident on a plane of single crystal at an angle θ and are diffracted according to Bragg's relation $2d \sin \theta = n\lambda$ where λ is the electromagnetic radiation, θ is the angle of diffraction, n is the order of diffraction and d is the lattice spacing of the crystalline sample. The diffracted X-rays are detected, processed and counted and the collection of intensities of the full set of planes in the crystal contains the complete structural information. The grown 4SAN crystal was subjected to single crystal X-ray diffraction study using ENRAF NONIUS CAD-4 X-ray diffractometer with MoK α ($\lambda=0.71069 \text{ \AA}$) radiation to find the crystal lattice parameters. The obtained lattice parameters of the grown 4SAN crystal are provided in the table 2. From the obtained data, it is confirmed that 4SAN crystal has monoclinic structure with the space group Cc. The number of molecular units per unit cell of the crystal $Z = 4$. The molecular weight of the sample is $M= 235.22$. The obtained values of lattice parameters of 4SAN crystal are observed to be well matched with the reported data [18]. The density of the grown 4SAN crystal was determined using the formula $\rho = M Z/NV$ where M is the molecular weight of the material used, Z is the number of molecules per unit cell, N is Avagadro's number and V is the volume of the unit cell. Hence, the density of the grown 4SAN crystal was calculated to be 1.634 g/cc by XRD method.

Table 2: XRD data for 4SAN crystal

Diffractometer	ENRAF NONIUS CAD-4
Radiation	MoK _α radiation
wavelength	0.71069 Å
Refinement method	Full matrix least square method
Temperature	293(2) K
Symmetry	Monoclinic
a	14.148(3) Å
b	8.182(3) Å
c	8.688(4) Å
α	90°
β	108.02 (2)°
γ	90°
Z	4
Volume of the unit cell	956.38 (4) Å ³

5. Microhardness studies

Hardness is a measure of material resistance to localized plastic deformation. The microhardness characterization is extremely important as far as the device fabrication is concerned. The smooth surface of 4SAN crystal was subjected to microhardness study at room temperature using a Vickers microhardness tester fitted with a diamond indenter. Loads of 25, 50, 75 and 100 grams were applied on the crystal for a fixed time interval of 10 seconds. The external work applied by the indenter is converted into a strain energy component proportional to the volume of the resultant impression and a surface energy component proportional to the area of resultant impression. The hardness of the crystal is determined using the relation

$$H_v = 1.8544 P/d^2$$

where P is the applied load, d is the length of indentation or impression, 1.8544 is a constant of a geometrical factor for the diamond pyramidal indenter. The calculated values of microhardness are presented in the figure 4 and the results show that the microhardness slightly increases initially and then it increases more when the applied load is more than 50 g. The phenomenon of testing the dependence of microhardness of a crystal with the applied load is called as indentation size effect. According to the normal indentation size effect (NISE), microhardness of crystal decreases with increase of the applied load and in reverse indentation size effect, hardness number increases with increase of the applied load. Hence, 4SAN crystal shows the reverse indentation size effect (RISE). The relation connecting the applied load and diagonal length of the indentation is given by Meyer's law $P=ad^n$, where n is the Meyer's index or work hardening coefficient. The Meyer's index is calculated from the slope of straight line drawn between log P and log d as shown in Fig.5 and the obtained value of n is 2.984 for 4SAN crystal. From careful observations on various materials, Onitsch and Hanneman pointed out that work hardening coefficient (n) lies between 1 and 1.6 for moderately hard materials and it is more than 1.6 for soft materials. Hence, 4SAN crystal belongs to the category of the soft

materials. According to Kick's law, n is less than 2 for normal NISE behavior, n is greater than 2 for RISE and the hardness is independent of applied load when n is equal to 2 [19-22].

Let the Meyer's law is to be written as $P=k_1d^n$ where k_1 is the material constant which can be obtained from the slope of the plot of P versus d^n (Fig.6). Since the material takes some time to revert to the elastic mode after every indentation, a correction factor x , a measure of dislocation density of the material is applied to the d value and the Kick's law is obtained as

$$P=k_2 (d+x)^2$$

On combining Meyer's law and Kick's law, the relation becomes

$$d^{n/2}=\left(\frac{k_2}{k_1}\right)^{1/2} d + \left(\frac{k_2}{k_1}\right)^{1/2} x$$

The slope of $d^{n/2}$ versus d yields $(k_2/k_1)^{1/2}$ and x is measured from the intercept on Y-axis (Fig.7). According to Kick's law, x is positive when $n < 2$ and negative for $n > 2$ [23]. The hardness parameters k_1 , k_2 and x were calculated for 4SAN crystal and are given in the table 3.

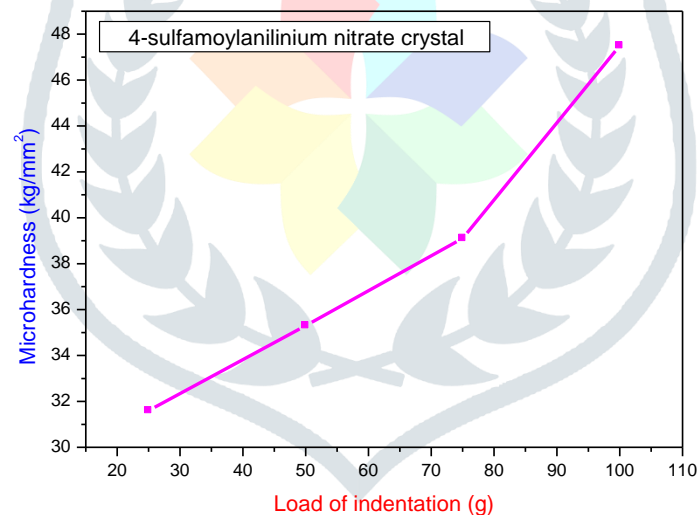


Fig.4: Plot of hardness value versus applied load for 4SAN crystal

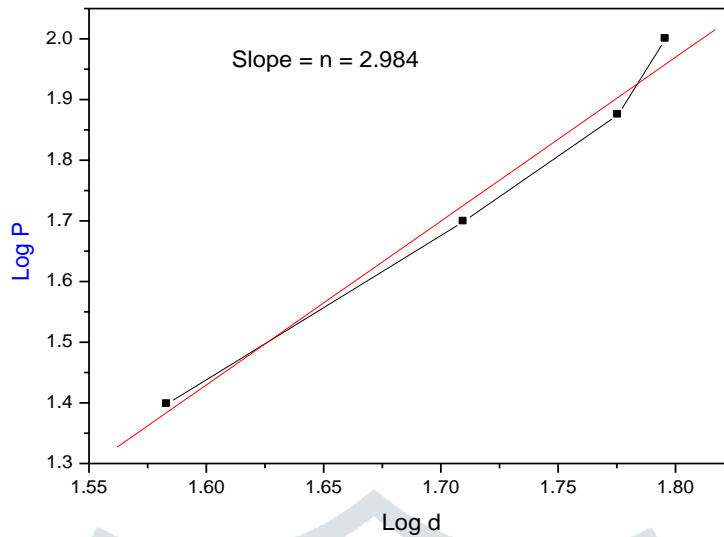


Fig.5: Plot of log P versus log d for 4SAN crystal

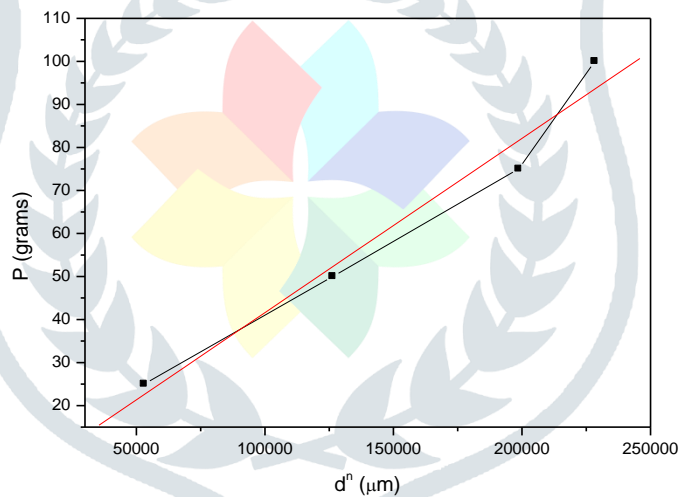


Fig.6: Plot of P versus d^n for 4SAN crystal

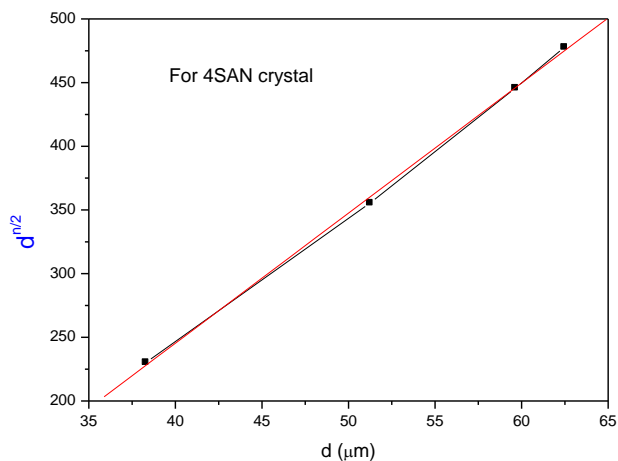


Fig.7: Plot of $d^{n/2}$ versus d for 4SAN crystal

Table 3: Hardness parameters of 4SAN crystal

Meyer's index	$k_1 \times 10^{11} \text{ kg/m}^2$	$k_2 \times 10^8 \text{ kg/m}^2$	x (μm)
2.984	4.057	2.582	- 3.281

6. Linear optical studies

The optical spectrum gives information about the electronic structure of the sample because the absorption of UV and visible light involves promotion of the electrons in the σ and π orbitals from the ground state to higher states. The UV-visible spectra were recorded using Lamda 35 spectrophotometer in the range of 200 nm to 800 nm and the recorded transmittance and absorbance spectra of 4SAN crystal are shown in the figures 8 and 9. From the results, it is evident that 4SAN crystal has UV cut-off wavelength at 295 nm and it is the intrinsic property of the sample. It is noticed that there is another cut-off wavelength at 240 nm and this may be due to indirect band gap nature of 4SAN crystal. In the visible region, 4SAN crystal has the high transmittance and this is necessary criteria for second harmonic generation (SHG). Also the absorbance spectrum indicates that 4SAN crystal has low absorbance in the visible region. The reflectance spectrum of 4SAN crystal is presented in the figure 10 and it gives that reflectance is low in the visible region and the negative value of reflectance indicates that 4SAN crystal has anti-reflection behaviour in the UV region. The optical absorption coefficient (α) was calculated using the following equation

$$\alpha = (2.303/d) * (\log_{10} (1/T))$$

where T is the transmittance and d is the thickness of the crystal. The variation of absorption coefficient with wavelength for 4SAN crystal is shown in the figure 11. Here it is observed that the behaviour of absorption

coefficient is similar to as that of absorbance of the sample and these values are used to draw the Tauc's plot of 4SAN crystal. Tauc's equation can be written as

$$\alpha h\nu = A(h\nu - E_g)^n$$

where E_g is optical band gap of the crystal, α is the absorption coefficient, h is the Planck's constant, ν is the frequency of light, n and A are constants. In a crystalline material, either direct or indirect optical transitions are possible depending on the band structure of the material. There will be a single linear region in direct transition and two linear portions in indirect transition. For a direct transition, $n=1/2$ or $3/2$ depending on whether the transition is allowed or forbidden in quantum mechanical sense. Similarly, $n=2$ or 3 for indirect allowed and forbidden transition respectively [24, 25]. The optical band gap was determined using Tauc's procedure by plotting $(\alpha h\nu)^{1/2}$ versus $h\nu$ as shown in Fig.12 and from the Tauc's plot, optical band gap of 4SAN crystal is found to be 4.17 eV. The extinction coefficient of 4SAN crystal was determined using the relation $K = (\alpha\lambda)/(4\pi)$ where α is the is absorption coefficient and λ is the wavelength of light and the plot of extinction coefficient with wavelength of 4SAN crystal is presented in the figure 13. The extinction coefficient is very low of the order of 10^{-5} and hence 4SAN crystal has low light energy loss. In the visible region of the spectrum, it is found that the extinction coefficient increases as the wavelength increases. From the linear optical studies, it is clearly observed that 4SAN crystal has high transmittance, low absorbance, low extinction coefficient and low reflectance in the visible region and hence this crystal possesses good optical behaviour for practical device applications [26-28].

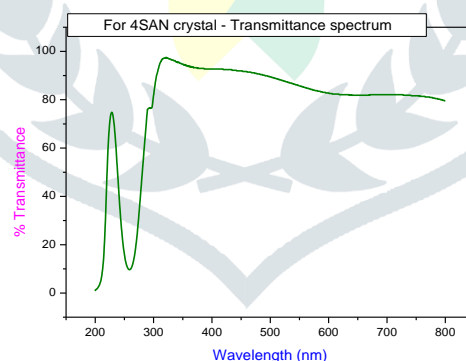


Fig.8: UV-visible transmittance spectrum of 4SAN crystal

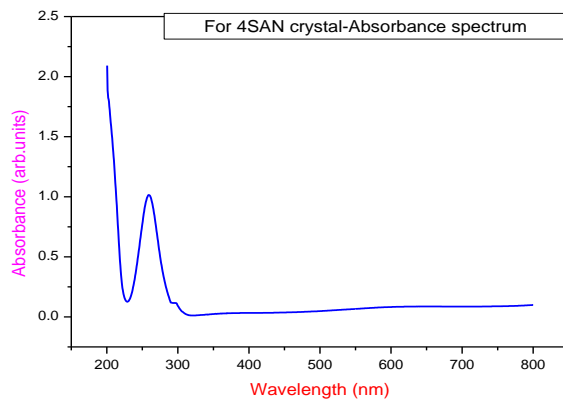


Fig.9: UV-visible absorbance spectrum of 4SAN crystal

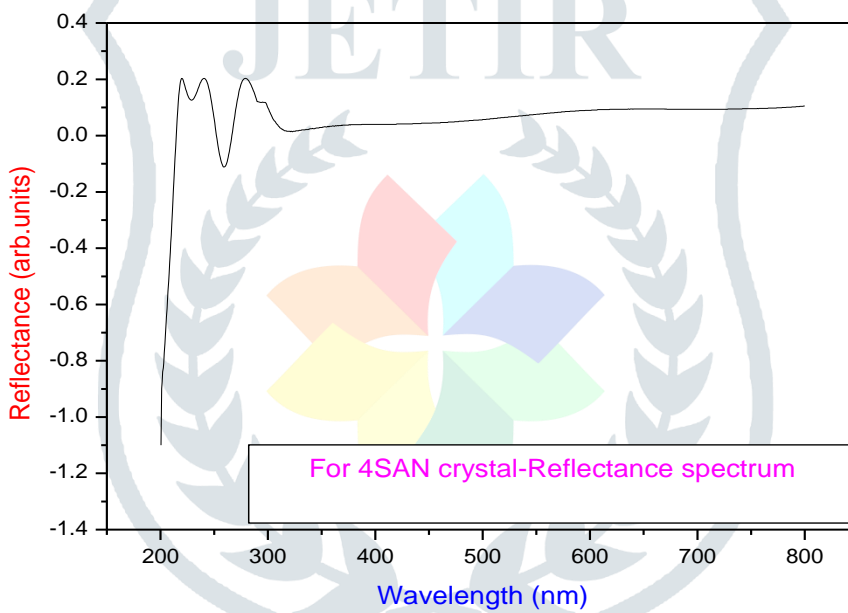


Fig.10: UV-visible reflectance spectrum of 4SAN crystal

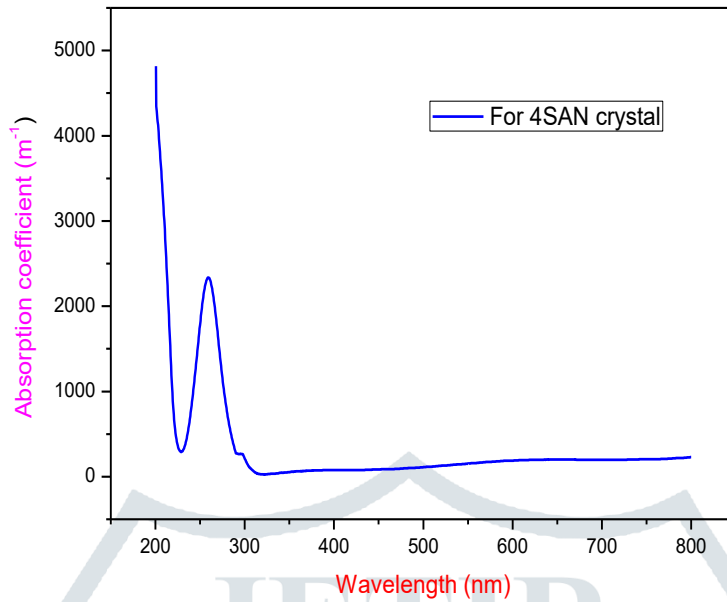


Fig.11: Variation of linear absorption coefficient with wavelength for 4SAN crystal

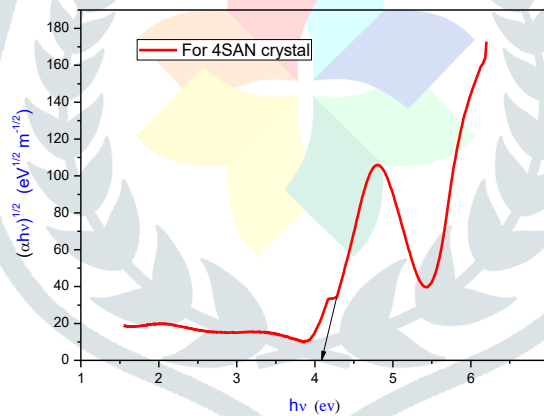


Fig.12: Tauc's plot for 4SAN crystal

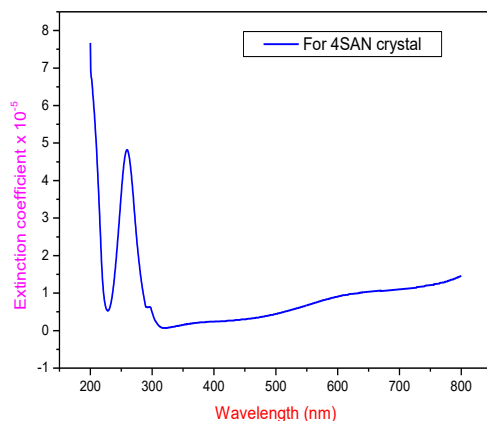


Fig.13: Variation of extinction coefficient with wavelength for 4SAN crystal

7. Conclusions

Single crystals of 4-sulfamoylanilinium nitrate were grown using sulphanilamide and nitric acid as the reactants. 4SAN crystal has the positive temperature coefficient of solubility. The functional groups like NH_2 , NO_3^- , SO_2 etc have been identified for the sample. 4SAN crystal crystallizes in monoclinic structure. Using the Tauc's plot, the optical band gap of 4SAN crystal is found to be 4.17 eV. The extinction coefficient of 4SAN crystal is observed to be very low of the order of 10^{-5} . The mechanical parameters like hardness, work hardening coefficient and other parameters of the sample were determined. Since 4SAN crystal has high transmittance, low absorbance, low extinction coefficient and low reflectance in the visible region, it could be useful in NLO applications.

Acknowledgement

The authors like to thank the staff members of various research institutions like Cochin University (Cochin), St. Joseph's college (Trichy) and NIT (Trichy) for collecting the research data.

References

1. P.N. Prasad, D.J. Williams, Introduction to Nonlinear Optical Effects in Molecules and Polymers, Wiley, New York, 1991.
2. H. Tanak, Int. J. Quant. Chem. 112 (2012) 2392–2402.
3. S.R. Marder, B. Kippelen, A.K.Y. Jen, N. Peyghambarian, Nature 388 (1997) 845– 851.
4. Wolff, M. E. Burger's Medicinal Chemistry, Part II. 4th ed.; Wiley & Sons: New York, Vol. 2, pp 1-40, 1979.

5. Mengelers, M. J. B.; Hougee, P. E.; Janssen, L. H. M.; Van Miert A. S. J. P. A. M. *J. Vet. Pharmacol. Therap.* 1997, 20, 276-283.
6. Cruz-Cabeza, A. J.; Bernstein, J. *Conformational Polymorphism. Chem. Rev.* 2014, 114, 2170-2191.
7. Martín-Islán, A. P.; Cruzado, M. C.; Asensio, R.; Sainz-Díaz, C. I. *J. Phys. Chem. B*, 2006, 110, 26148–26159.
8. Adsmond, D. A.; Frant, D. J. W. *J. Pharm. Sci.* 2001, 90, 2058-2077.
9. Lee, Y. J., Park, Y. J. *J. Korean Chem. Soc.* 25, 219-227.
10. Rambaud, J.; Roques, R.; Declercq, J. P.; Germain, G.; Sabon, F. *Bull. Soc. Chim. Fr.* 1981, 153-160.
11. Badiiaa Essghaier, Amani Naouar, Jawher Abdelhak, Mohamed Faouzi Zid, Najla Sadfi-Zouaoui, *Microbiological Research*, 169, 2014, 504-510.
12. Jaroslav Nyvlt, Rudolf Rychly, Jaroslav Gottfried, Jirina Wurzelova, J. *Crystal Growth*, 6(2)(1970)151-162.
13. N.P.Rajesh, P.Santhana Raghavan, P.Ramasamy, C.W.Lan and J.Chin, *Inst. Chem. Engrs.* 33 (2002) 325-331.
14. Albert N. L., Keiser W.E. and Szymanski H. A., *IR theory, Practice of IR Spectroscopy* (Plenum Press, New York, 1973).
15. Griffiths P. R. and De Hoseth J. A., *Fourier Transform Infrared Spectroscopy* (Wiley, Chichester, 1986).
16. Chandran Muthuselvi, Murugesan Pandeewari and Sankara Sabapathy Pandiarajan, *Asian J. Appl.Sci.*, 10 (2017) 170-178.
17. Peter R. Griffiths; James A. De Haseth (2007). *Fourier Transform Infrared Spectrometry* (2nd ed.). John Wiley & Sons.
18. S.Pandiarajan, S.Balasubramanian, B.Ravikumar, S.Athimoolam, *Acta Cryst. E*67,(2011) o2788.
19. .Gong J and Li Y, *J. Mater. Sci.*, 35 (2000) 209.
20. Meyer E and Otsch Z Ver, *Ing.*, 52 (1908) 645.
21. .Onitsch E M, *Mikroscopia*, 2 (1947) 131.
22. .Hanneman M., *Metall. Manch*, 23 (1941) 135.
23. Dinakaran S, Sunil Verma, Justin Raj, Mary Linet, Krishnan and Jerome Das, *J. Crystal Growth and Design*, 9(1) (2009) 151.
24. Mary Linet J and Jeromedos S, *Mater. Chem. and Phys.*, 126 (2010) 886.
25. J. Tauc, R. Grigorovici, A. Vancu, *Phys. Status Solidi B* 15 (1966) 627–637.
26. .P. Rekha, G. Peramaiyan, M. Nizam Mohideen, R. Mohan Kumar, R. Kanagadurai, *Spectrochim. Acta Part A*, 139 (2015) 302–306.

27. G. Shanmugam, K. Thirupugalmani, V. Kannan, S. Brahadeeswaran, Spectrochim. Acta Part A 106 (2013) 175–184.
28. V. Subhashini, S. Ponnusamy, C. Muthamizhchelvan, B. Dhanalakshmi, Opt. Mater. 35 (2013) 1327–1334.

